Adsorption (2013) 19:803–811
DOI 10.1007/s10450-013-9522-7

A hydrogen sorption study on a Pd-doped CMK-3 type ordered mesoporous carbon

D. Giasafaki · G. Charalambopoulou · A. Bourlinos · A. Stubos · D. Gournis · Th. Steriotis

Received: 31 October 2012 / Accepted: 16 February 2013 / Published online: 5 March 2013

Abstract An ordered mesoporous carbon of CMK-3 type was prepared and modified by metal doping with Pd nanoparticles. The hydrogen sorption performance of the pristine and composite materials was studied at different temperature and pressure conditions in order to provide insight into the underlying storage mechanism. It was shown that metal doping can lead to enhanced hydrogen storage at 298 K as a result of a weak chemisorption process initiated by the so-called "spillover" effect.

Keywords Hydrogen storage · Ordered mesoporous carbons · Metal doped carbons · Spillover

1 Introduction

Despite the technological hurdles, the attractiveness of solid storage of hydrogen, still considered to have several advantages over compression and liquefaction technologies, continues to spark intense research efforts pursuing safe and efficient material-based solutions to store energy, both for stationary and mobile applications. High surface area carbon-based sorbents are among the most widely investigated materials, due to the plethora of available nanoporous systems with low density, high pore volume and attractive cost (Texier-Mandoki et al. 2004; Xia et al. 2007, 2008; Ding and Yakobson 2011). The interaction between hydrogen and pure carbon surfaces is weak leading to H_2 molecular physisorption which can be useful for storage only at temperatures around that of liquid nitrogen (Gogotsi et al. 2009; Guo and Gao 2010; Jiménez et al. 2012; Zhao et al. 2012). The adsorption performance of such systems at room temperature and normal operating pressures (e.g. below 200 bar) still remains far below the desirable targets for practical storage applications (Wang et al. 2009; Jiang et al. 2010; Kockrick et al. 2010; Wang et al. 2010; Wang and Yang 2010; Yang et al. 2006; Anbia and Mandegarzad 2012; Zhao et al. 2012) as defined by the US Department of Energy. The broad compositional and structural diversity of carbon-based materials along with their amenability to functionalisation, has triggered the search of strategies to increase appropriately the strength of hydrogen binding in order to allow adsorption at temperatures near ambient and/or improve capacity. A number of methodologies including optimization of the porous system geometry, chemical surface modifications and doping, have been explored to this direction (Li et al. 2005; Li and Yang, 2007; Lysenko et al. 2009; Li and Lueking 2011; Lee and Park 2011; Yang et al. 2011a; Han et al. 2012; Lee and Park 2012; Wang and Yang 2012; Zhao et al. 2012).

An approach that has been the subject of massive work in the last few years involves the decoration of carbon matrices with transition metals, giving rise to synergistic effects such as the so-called "spillover" catalytic mechanism (Yang et al. 2006), or Kubas-type binding (Contescu et al. 2011). Among the variety of transition metals that have been examined, particular attention has been given to

D. Giasafaki · G. Charalambopoulou (✉) · A. Stubos · Th. Steriotis
National Center for Scientific Research "Demokritos", 15310 Ag. Paraskevi Attikis, Athens, Greece
e-mail: gchar@chem.demokritos.gr

D. Giasafaki · D. Gournis
Department of Material Science Engineering, University of Ioannina, 45110 Ioannina, Greece

A. Bourlinos
Department of Physics, University of Ioannina, 45110 Ioannina, Greece

palladium. Pd can easily be produced as clean, stable and well-defined nanoparticles (Toebes et al. 2001), while the well-studied Pd-H isotherms show that a significant amount of hydrogen can be absorbed even at low pressures and desorbed in vacuum at 393 K (Eastman et al. 1993). As for the prevailing mechanism, Kubas-type complexes can be formed through the molecular polarization and multiple σ-bonding of H_2 molecules with d orbitals of single transition metal atoms (Kubas 1988) or ions (Niu et al. 1992). However in most cases transition metals tend to form robust aggregates, hindering the occurrence of distinct metal atoms, and thus a mechanism such as that of hydrogen "spillover" is more favorable. This is a weak chemisorption process that occurs at moderate temperature (e.g. 298 K) and involves the catalytic dissociation of hydrogen molecules on the metal sites, followed by the migration of atomic H to the surface of the inert support and the surface diffusion/sorption of H atoms (Wang and Yang 2010; Psofogiannakis et al. 2011; Jiménez et al. 2012). The result is in general a much higher uptake than the one expected for the metal catalyst or high-surface area adsorbent alone.

Room temperature hydrogen storage capacities reported for a large number of spillover materials have been widely dispersed, and have lead to controversy about the accuracy and reproducibility of the results but also the very existence of hydrogen "spillover" (Hirscher 2010; Prins 2012). Recently it was announced that an international round-robin exercise has confirmed that "spillover" can increase excess adsorption at room temperature by at least 15 % (Stetson 2012). The conclusions were also based on spectroscopic evidence of reversible substrate-hydrogen interactions. Inelastic neutron and small-angle neutron scattering but also theoretical studies have shown that spillover from metal particles to a carbonaceous support is in principle energetically possible (Mitchell et al. 2003; Psofogiannakis and Froudakis 2009; Tsao et al. 2010; Psofogiannakis et al. 2011; Prins 2012; Wang and Yang 2012). Nevertheless, the mechanistic details of "spillover" remain poorly understood since the process depends strongly on the synthesis and the structure/composition of the composite materials.

As hydrogen spillover involves the migration of the active hydrogen species from the metal sites onto the adjacent surface of the receptors, it is desired to maximize the contacts between the two components (Wang et al. 2010). Additionally, the catalytic centers should be always exposed to the hydrogen molecules, even after repetitive cycles. In this respect, apart from the size, loading amount and dispersion of the metal particles, the optimization of the pore geometry, accessibility and connectivity of the carbon support is also highly important (Yang et al. 2011a).

Nanocasting is an effective approach to control the porous structure especially of carbon-based sorbents (which are difficult to obtain by typical liquid-precursor routes), as it can provide well-defined porous networks with adjustable micro- and meso- porosity (Ryoo et al. 1999; Ryoo et al. 2001; Xia et al. 2008; Lee and Park 2011; Anbia and Mandegarzad 2012). It is based on the infiltration of a (usually silica-based) mesoporous mold with a carbon precursor solution that can be polymerized upon heat treatment, carbonization of the composite and removal of the template. One of the most widely-studied ordered mesoporous carbons is the one designated as CMK-3 (Ryoo et al. 1999). This type of carbon possesses a hexagonal interconnected ordered structure, uniform mesopores, a large surface area and a noticeable volume of micropores. Along with its high chemical stability and durability, this material offers a suitable model for studying the hydrogen "spillover" mechanism.

In the present work an ordered mesoporous CMK-3 type carbon was prepared and decorated with Pd nanoparticles. The composite material was characterised with regard to its morphological, structural and textural properties, while hydrogen sorption measurements at different temperature and pressure conditions showed that the synergy between the metal nanoparticles and the carbon support play indeed a considerable role in the overall hydrogen storage performance at room temperature.

2 Experimental

2.1 Materials

A typical nanocasting procedure was adapted (Ryoo et al. 1999; Jun et al. 2000) for the synthesis of the CMK-3 type ordered mesoporous carbon, using SBA-15 ordered mesoporous silica as template and sucrose as the carbon precursor.

SBA-15 was prepared according to a well established method (Zhao et al. 1998a; Shin et al. 2001; Lu et al. 2005), using triblock copolymer $EO_{20}PO_{70}EO_{20}$ (Pluronic P123, Aldrich) as the surfactant agent, and tetraethylorthosilicate (TEOS 98 %, Aldrich) as the silica source at a composition of 4 g of P123:0.041 mol TEOS:0.24 mol HCl:6.67 mol H_2O. Aiming to obtain a carbon sample with the inverse structure (denoted hereafter as *C3*), the SBA-15 mesoporous silica was impregnated twice with an acidic sucrose solution, subsequently carbonised by pyrolysis up to 900 °C under N_2 gas flow, followed by etching of the silica framework using HF at room temperature.

The as synthesised *C3* sample was treated by an aqueous solution of anhydrous $PdCl_2$ (60 % Pd, Fluka), for 24 h under stirring at room temperature, in order to acquire the

metal-doped carbon materials, according to previously reported procedures (Giasafaki et al. 2011, 2012), using $NaBH_4$ as reducing agent. The exact content of Pd in the doped sample was determined by thermogravimetric analysis (TGA) measurements. After the complete combustion of organic components and carbon burn-off (it should be noted that the analysis of the pristine C3 carbon showed no residual), the remaining mass at 1,200 °C was entirely attributed to palladium oxide, translating to 11 wt% loading of Pd.

2.2 Methods

TGA measurements were performed on appr. 10 mg of each sample using a SETARAM SETSYS Evolution 18 Analyser, in the range of 25–1,200 °C, with a heating rate of 20 °C/min in an Al_2O_3 crucible under air flow (16 ml/min). Purging was applied well before initiating thermal analysis to efficiently control the sample environment within the furnace. In addition buoyancy corrections were made by subtracting the baseline collected by a blank TGA run with an empty crucible.

The surface morphology of the materials as well as the dispersion of the metal particles were studied using a Jeol JSM 7401F Field Emission Scanning Electron Microscope (SEM) equipped with Gentle Beam mode, while Transmission electron microscope (TEM) images were obtained from a high resolution JEM-2100 instrument equipped with LaB6 filament.

IR spectra were obtained using a Thermo Scientific Nicolet 6700 FTIR equipped with a N_2 purging system and a LN_2-cooled wide range Mercuric Cadmium Telluride detector.

The XRD patterns of all samples were recorded on a Rigaku R-AXIS IV Imaging Plate Detector mounted on a Rigaku RU-H3R Rotating Copper Anode X-ray Generator ($\lambda = 1.54$ Å).

The textural properties of the micro-mesoporous pristine and Pd-doped carbon materials were evaluated by N_2 adsorption/desorption measurements at 77 K on a volumetric gas adsorption analyser (Autosorb-1-MP, Quantachrome). The samples ($\sim$50 mg) were appropriately outgassed ($\sim$48 h at 250 °C) under high vacuum (10^{-6} mbar), while ultra-pure N_2 (99.9999 %) was used. The specific surface area values were calculated by the Brunauer–Emmett–Teller (BET) method in the relative pressure range between 0.07 and 0.15, following the BET consistency criteria (ISO 9277:2010). The micropore volumes and the micropore surface areas were determined using the Dubinin-Radushkevich (DR) approximation. The pore size distributions were deduced applying the NLDFT (Non-Local Density Functional Theory) method for slit/cylindrical shaped pores of carbon materials, provided by Quantachrome data reduction software, version 2.01.

The hydrogen sorption isotherms of the materials were determined at 77 and 298 K up to 22 bar, using a PCTPro-2000 automatic volumetric system (SETARAM) and ultra-pure (99.9999 %) hydrogen gas. A certain amount (appr. 130 mg) of each sample was placed in a stainless steel sample cell closed with a metal seal and degassed under high vacuum (10^{-6} mbar) at 250 °C for at least 24 h. Volume calibrations with helium gas were performed prior to measurement, also using inert non-sorbing Pyrex samples having the same skeletal volume with the carbon materials examined.

A custom-made sorption–desorption rig, coupled with a mass spectrometer (MS) was used for a series of controlled desorption measurements. The experimental setup was composed of a quartz sample cell connected with a turbo pump and the inlet capillary of a quadrupole mass spectrometer (OmniStar GSD 301 O1, Pfeiffer). After appropriately outgassing each sample (at 250 °C for 24 h under high vacuum), this was exposed to 50 mbar of pure D_2 for 24 h, to reach equilibrium. In order to investigate the interactions of the sorbed gas with the carbon surface of the materials, the temporal profiles of ion currents for *m/z* values corresponding to H_2, HD, D_2, H_2O, HDO, D_2O and fragments were recorded. A second and third cycle of sorption–desorption analysis through MS was performed, after intermediate outgassing at 250 °C under high vacuum.

3 Results and discussion

3.1 Material characterisation

The SEM image of Fig. 1 shows the macrostructure of the doped *C3Pd* material, consisting of agglomerated rod-like

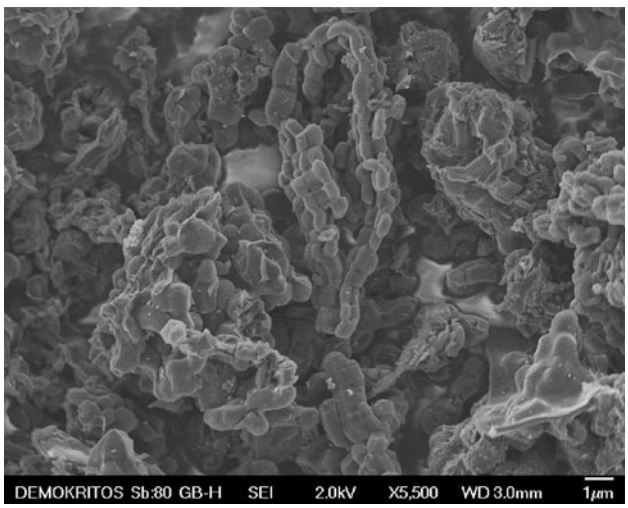

Fig. 1 SEM image of the doped *C3Pd* material (scale: 1 μm)

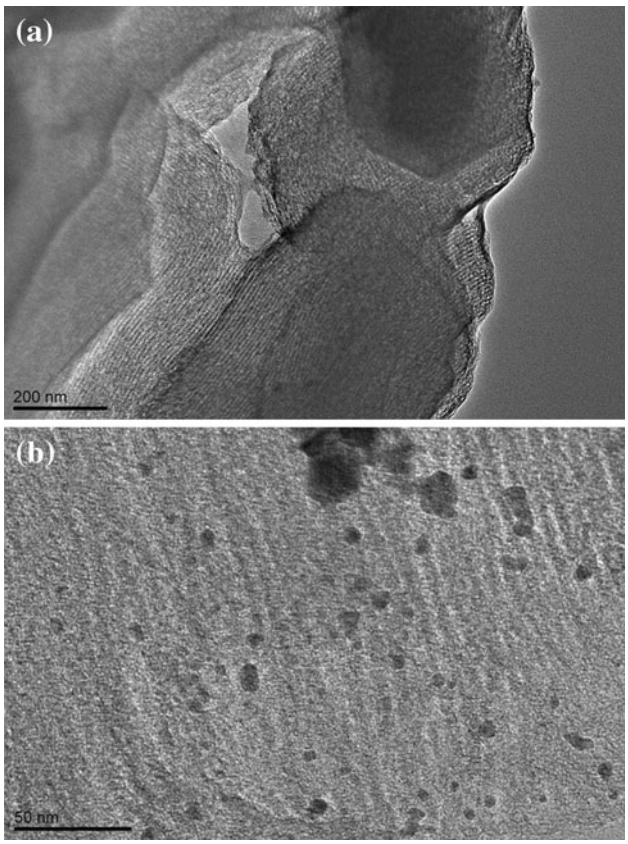

Fig. 2 TEM images of **a** *C3* pristine carbon (scale: 200 nm) and **b** *C3Pd* doped material (scale: 50 nm)

elongated carbon particles, typical for CMK-3 type carbons.

The microstructure of the pristine and Pd-doped carbon samples is characterized by a well-organised pore structure as revealed by TEM images (Fig. 2), depicting stripe-like patterns formed by the black linear arrays of the carbon nanorods separated by the white parallel aligned channels. The 2D periodic hexagonal mesostructure was maintained after metal doping, whereas as it can be seen in Fig. 2b, some metal particles (dark spots) are embedded in the carbon pores, while aggregates outside the mesochannels are also observed.

Furthermore the FTIR spectra of both the pristine and Pd-doped samples (Fig. 3) are quite similar and show some features in the range 1,020–1,220 cm^{-1} that might be ascribed to the stretching vibrations of C–O bonds (Fanning and Vannice 1993; Jaramillo et al. 2010). This suggests that the surface of the materials has a certain oxygen content which is not affected by the incorporation of the metal nanoparticles.

Metal doping did neither affect the ordered mesoporous structure of the pristine *C3* carbon as shown by the X-ray diffraction patterns of Fig. 4, in consistency with the TEM analysis. In the range 0–4° the pristine and Pd-doped samples exhibited intense peaks at around $2\theta = 1.2°$ attributed

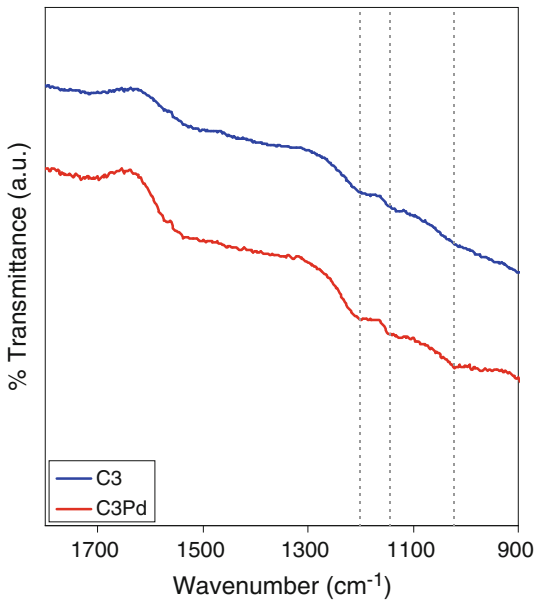

Fig. 3 FTIR spectra of pristine carbon *C3* and its doped analogue *C3Pd* (the *dotted lines* are guiding the eye for the features observed in the range 1,020–1,220 cm^{-1})

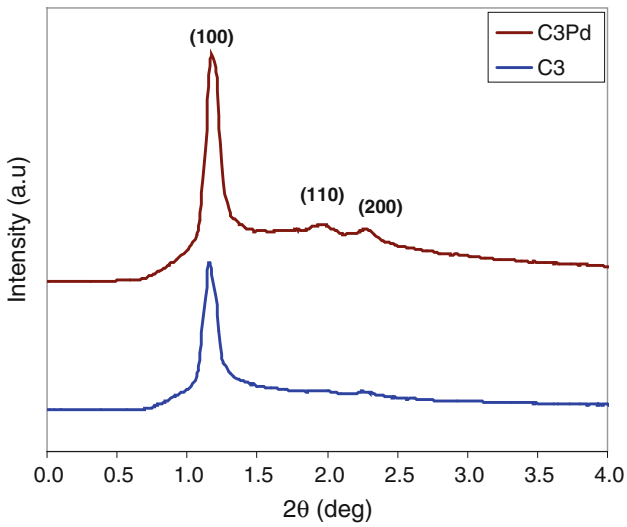

Fig. 4 Small-angle XRD patterns of the pristine carbon *C3* and its doped analogue *C3Pd*

to (100) reflection, as well as weaker peaks centered at about $2\theta = 2°$ and 2.3° that can be indexed to (110) and (200) reflections, respectively. The patterns suggest that both samples possess a long-range ordering, since these three peaks are characteristic of the porous materials organized in hexagonal arrays (p6 mm space group) (Zhao et al. 1998b).

The wide-angle XRD pattern (Fig. 5) of the Pd-doped material, exhibits well-resolved peaks at approximately $2\theta = 40°$, 47°, 68°, 82°, 87° corresponding to the characteristic diffraction peaks of the face-centered cubic structure of palladium. These results highlight the biphasic

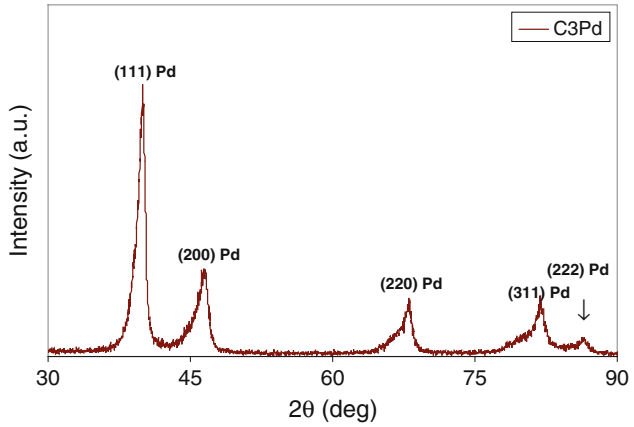

Fig. 5 Wide-angle XRD pattern of the Pd-doped carbon material *C3Pd*

nature of the doped carbon and confirm the successful incorporation of metallic Pd. The mean size of the Pd nanoparticles was estimated to be around 15 nm by applying Scherrer's formula for the (111) diffraction peak.

The textural properties of the pristine and Pd-doped materials were determined by N_2 adsorption–desorption measurements at 77 K. As shown in Fig. 6 all samples exhibited type-IV isotherms with less pronounced capillary condensation steps (pointing to broader pore size distributions) and hysteresis loops, typical of mesoporous materials with slit-shaped pores.

The pore size distributions of the materials as obtained from the NLDFT-based analysis are illustrated in the inset of Fig. 6 and reveal in all cases narrow peaks in the range of 4–7 nm reflecting primary mesopores, but also pronounced microporosity centered around 1.2–1.5 nm.

The comparison of the textural properties of the pristine and Pd-doped samples summarized in Table 1, shows that the metal doping procedure has a certain effect on the pore structure of the *C3* carbon. *C3Pd* depicts reduced surface area and pore volume compared to *C3* indicating that some pores (mainly mesopores) of the pristine carbon matrix might have been partially blocked from the incorporation of the metal nanoparticles.

3.2 Hydrogen sorption properties

The hydrogen sorption isotherms of the pristine and the doped carbon materials at 77 K and up to 22 bar are illustrated in Fig. 7. Both samples showed full reversibility with almost no hysteresis loop, demonstrating that physical adsorption dominates. The two curves have similar shape and follow the same trend with the N_2 adsorption isotherms at low pressures. Indeed the higher-surface-area/larger-pore-volume *C3* sample exhibits a somewhat higher saturation hydrogen adsorption capacity than its doped

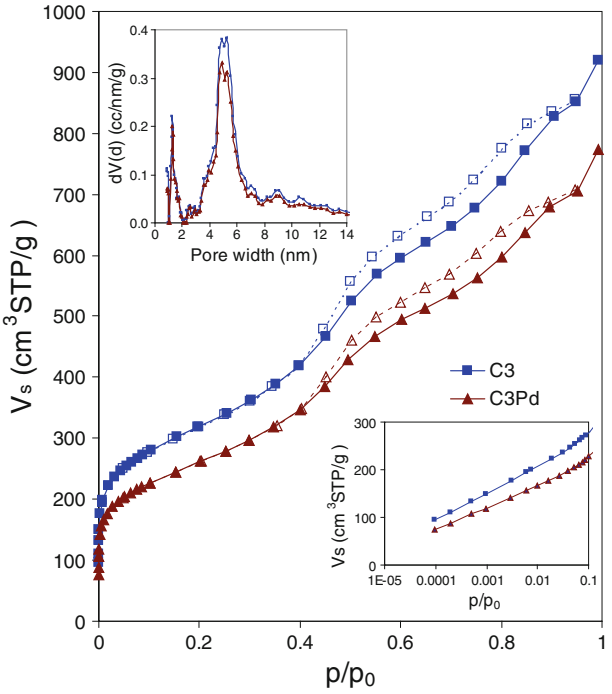

Fig. 6 N_2 sorption–desorption isotherms at 77 K of the pristine carbon material *C3* and its Pd-doped analogue *C3Pd* (*full symbols/continuous line*: sorption, *empty symbols/dashed line*: desorption). The *insets* show the pore size distributions (*up-left*) of the materials as obtained from the NLDFT-based analysis and the expansion of the isotherms (*top-right*) at low relative pressures (logarithmic scale)

analogue *C3Pd*. This indicates that the pore properties have a certain impact on H_2 uptake at 77 K, in consistency with relevant studies having investigated the role of pore volume and surface area on hydrogen adsorption for a large variety of modified carbons (De la Casa-Lillo et al. 2002; Texier-Mandoki et al. 2004; Kowalczyk et al. 2005; Xia et al. 2007; Armandi et al. 2008; Nishihara et al. 2009; Guo and Gao 2010; Kockrick et al. 2010; Zheng et al. 2010; Salvador et al. 2011; Yang et al. 2011b; Yang et al. 2012). Even though in most cases a direct relationship between the adsorbed hydrogen and these textural parameters has been proposed, the exact correlation still remains controversial (Armandi et al. 2008; Xia et al., 2008; Gogotsi et al. 2009; Guo and Gao 2010). Experimental results (Armandi et al. 2008; Yang et al. 2012) as well as theoretical predictions (Gogotsi et al. 2009) have for example suggested that Chahine's rule (Panella et al. 2005) is not universal, giving more emphasis to the presence of small micropores rather than to the high surface area or large total pore volume.

Contrary to 77 K, pore properties do not have any significant effect on hydrogen adsorption at 298 K, as also shown by the performance of the pristine and Pd-doped carbon samples, presented in Fig. 8. Regardless the porosity loss produced after metal incorporation, the

Table 1 Textural properties of the pristine *C3* and doped *C3Pd* sample (*BET* Brunauer–Emmett–Teller approach, *DR* Dubinin-Radushkevich approach, S_{BET} BET surface area, S_{DR} DR surface area, V_{micro} micropore volume deduced from DR method, V_{meso} mesopore volume, *TPV* total pore volume (at p/p0 = 0.95), *Microporosity* V_{micro}/TPV percentage, *NLDFT* mean pore size based on NLDFT analysis)

Sample	S_{BET} (m^2/g)	S_{DR} (m^2/g)	*TPV* (cm^3/g)	V_{micro} (cm^3/g)	V_{meso} (cm^3/g)	Microporosity (%)	NLDFT (nm)
C3	1,145	1,159	1.32	0.41	0.91	31	5.3
C3Pd	942	946	1.10	0.34	0.77	30	4.9

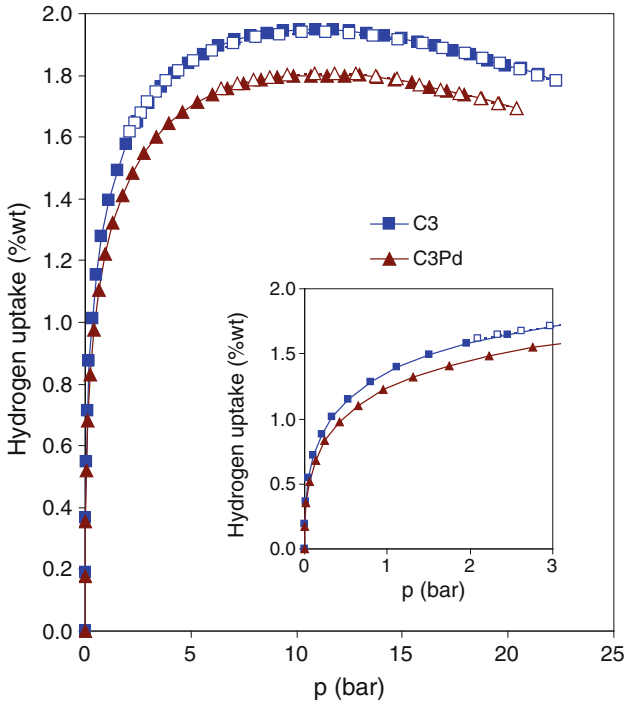

Fig. 7 High pressure H_2 sorption–desorption isotherms at 77 K for the pristine *C3* carbon material and its doped analogue *C3Pd* (*full symbols/continuous line*: sorption, *empty symbols/dashed line*: desorption). The *inset* shows an expansion of the H_2 sorption isotherms at low pressures

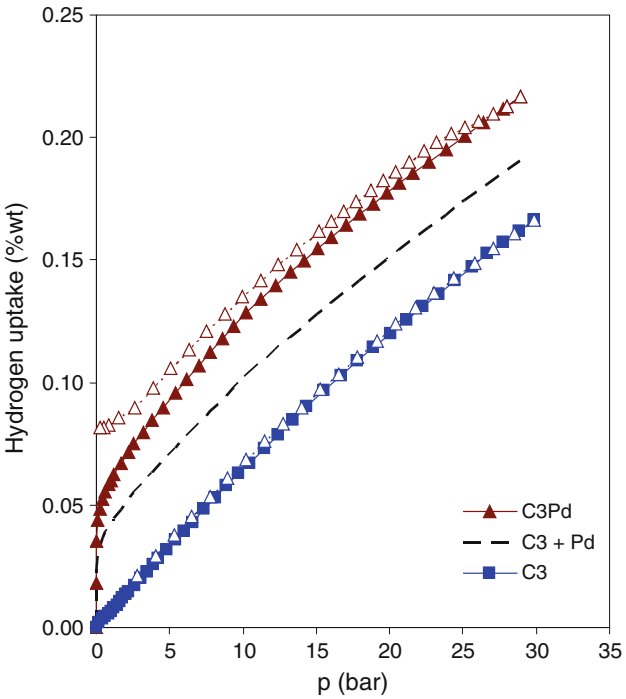

Fig. 8 High-pressure H_2 sorption–desorption isotherms at 298 K for the pristine *C3* carbon material and its doped analogue *C3Pd* (*full symbols/continuous line*: sorption, *empty symbols/dashed line*: desorption). The *dot-dashed line* represents the purely additive effect of the carbon support and Pd content

hydrogen sorption capacity was improved (Anbia and Mandegarzad 2012; Jiménez et al. 2012). While the parent *C3* material displayed a rather low uptake, the metal doping of the carbon surface altered the hydrogen adsorption behavior presumably by modifying both the pore texture and surface interactions with hydrogen (Stein et al. 2009). Indeed for the pristine carbon *C3*, the capacity increased linearly with pressure without reaching a maximum value, while no hysteresis loop was observed. The doped sample exhibited a significantly higher uptake than *C3*, which cannot be explained on the basis of the differences between the respective surface areas and pore volumes. In addition, a distinct hysteresis loop was observed indicating deviation from pure physisorption effects (Ioannatos and Verykios 2010; Jiménez et al. 2012).

The improved performance of the Pd-doped carbon at 298 K can be attributed to the synergy between the metal and carbon components of the composite system. The enhanced uptake may be the combined result of different mechanisms, i.e. sorption on the carbon support (which is not negligible as also shown by the *C3* H_2 sorption isotherm), hydride formation in large Pd particles (that could be responsible for the rapid hydrogen uptake observed at very low pressures), and hydrogen spillover from the Pd catalytic sites to the carbon surface. Assuming that the composite's metal content completely converts to $PdH_{0.7}$ upon exposure to hydrogen, the simple addition of the sorption expected from the Pd nanoparticles and the carbon alone (deduced by: 0.89 × H_2 uptake of carbon + 0.11 × H_2 uptake of $PdH_{0.7}$ for each equilibrium pressure point at

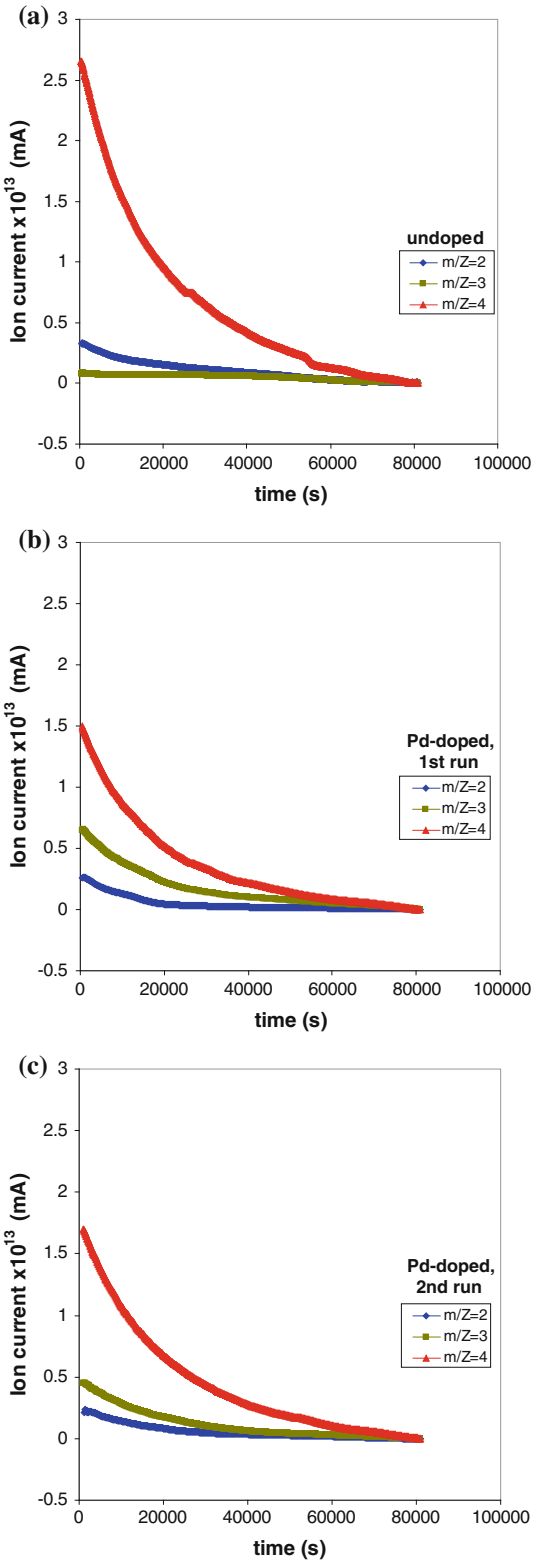

Fig. 9 D_2 desorption-MS data (298 K) for **a** the pristine *C3* carbon, **b** the doped *C3Pd* and **c** the doped *C3Pd* after a second sorption–desorption cycle

298 K) results in a lower uptake (dot-dashed line in Fig. 8) than that actually observed for the *C3Pd* material. This contribution is however small compared to the overall capacity enhancement. In this context, it seems that hydrogen "spillover" might be mainly responsible for the improved performance of the Pd-doped mesoporous carbon building on the dissociative metal catalytic sites.

In order to further investigate the interaction of hydrogen with the surface of the Pd/carbon composite a series of low pressure D_2 sorption–desorption experiments coupled with mass spectroscopy, were performed. After appropriate outgassing of the *C3* and *C3Pd* samples, these were exposed to 50 mbar of D_2 at room temperature for 24 h. After reaching equilibrium, the system was evacuated through a mass spectrometer, recording the temporal profiles of the ion intensities at $m/z = 2, 3, 4, 18, 19, 20$ attributed to H_2, HD, D_2, H_2O, HDO, D_2O, respectively.

Figure 9a presents the MS signals of H_2, HD, and D_2 obtained from the desorption of the undoped sample which can be used as reference. As expected, the primary signal in this case is that of D_2, while small amounts of hydrogen impurities are also detected. On the other hand, Fig 9b presents the desorbed species from the doped sample. In this case the D_2 signal reduces markedly, giving rise to a new signal assigned to HD. HD concentration decreases after a second sorption–desorption cycle (Fig. 9c), while the detected D_2 increases, still not reaching the initial amount. These results indicate that deuterium reaches the carbon surface in atomic form, in support of the "spillover" theory. The whole process could probably be explained as follows. Atomic species can be formed from the dissociative chemisorption of D_2 on the catalytic centers (Pd nanoparticles). Atomic deuterium then spills over onto the surface of the carbon support, spreads and bonds with active sites of the surface, while some atoms recombine on the surface or the metal centers and desorb as molecules (Takagi et al. 2005; Lachawiec and Yang 2008; Lachawiec and Yang, 2009; Psofogiannakis et al.2011). As the D atoms migrate on the carbon surface, some of them reach regions containing H atoms which can thus be substituted. The released H species, being mobile and light, can bond with other H atoms to form H_2, D atoms to form HD or even surface oxygen groups giving H_2O, HDO and/or D_2O (the pertinent signals were however negligible in our case). The above process leads to a progressive depletion of hydrogen from the carbon surface, as suggested by the decrease of the HD signal as well as a higher D_2 intensity (still less than the initial amount) observed during the second cycle (Fig. 9c).

4 Conclusions

High-pressure hydrogen sorption measurements on pristine and a Pd-doped ordered mesoporous carbon showed that although pore properties play a significant role for the performance of the system at 77 K, the storage capacity at ambient temperature can be greatly affected by the presence of metal catalytic sites. The metal-free and doped samples exhibit comparable hydrogen sorption performance at 77 K, which is moreover consistent with the respective textural properties. At room temperature the pristine carbon has a rather low hydrogen storage capacity which is however significantly enhanced upon metal-doping. The respective uptake cannot be explained by simply adding the contributions from the Pd hydride formation and the sorption on the carbon support. In-situ sorption–desorption/MS results provide qualitative, yet sufficient, evidence of the prevailing mechanism involving hydrogen dissociation-spillover, subsequent diffusion of the H atoms on the carbon surface and recombination to gas molecules.

Acknowledgments The authors wish to acknowledge partial support of the Research Funding programme Thales "Development of novel nanoporous materials for hydrogen storage" (Contract No. 3580), co-financed by the European Union (European Social Fund – ESF) and Greek national funds through the Operational Program "Education and Lifelong Learning" of the National Strategic Reference Framework (NSRF).

References

Anbia, M., Mandegarzad, S.: Enhanced hydrogen sorption on modified MIL-101 with Pt/CMK-3 by hydrogen spillover effect. J. Alloys Compd. **532**, 61–67 (2012)

Armandi, M., Bonelli, B., Karaindrou, E.I., Areán, C.O., Garrone, E.: Post-synthesis modifications of SBA-15 carbon replicas: improving hydrogen storage by increasing microporous volume. Catal. Today **138**, 244–248 (2008)

Contescu, C.I., van Benthem, K., Li, S., Bonifacio, C.S., Pennycook, S.J., Jena, P., Gallego, N.C.: Single Pd atoms in activated carbon fibers and their contribution to hydrogen storage. Carbon **49**, 4050–4058 (2011)

De la Casa-Lillo, M.A., Lamari-Darkrim, F., Cazorla-Amorós, D., Linares-Solano, A.: Hydrogen storage in activated carbons and activated carbon fibers. J. Phys. Chem. B **106**, 10930–10934 (2002)

Ding, F., Yakobson, B.I.: Challenges in hydrogen adsorptions: from physisorption to chemisorption. Front. Phys. **6**, 142–150 (2011)

Eastman, J.A., Thompson, L.J., Kestel, B.J.: Narrowing of the palladium-hydrogen miscibility gap in nanocrystalline palladium. Phys. Rev. B **48**, 84–92 (1993)

Fanning, P.E., Vannice, M.A.: A Drifts Study of the Formation of Surface Groups on Carbon by Oxidation. Carbon **31**, 721–730 (1993)

Giasafaki, D., Bourlinos, A., Charalambopoulou, G., Stubos, A., Steriotis, T.: Synthesis and characterisation of nanoporous carbon–metal composites for hydrogen storage. Microporous Mesoporous Mater. **154**, 74–81 (2012)

Giasafaki, D., Bourlinos, A., Charalambopoulou, G., Stubos, A., Steriotis, T.: Nanoporous carbon—metal composites for hydrogen storage. Cent. Eur. J. Chem. **9**, 948–952 (2011)

Gogotsi, Y., Portet, C., Osswald, S., Simmons, J.M., Yildirim, T., Laudisio, G., Fischer, J.E.: Importance of pore size in high-pressure hydrogen storage by porous carbons. Int. J. Hydrogen Energy **34**, 6314–6319 (2009)

Guo, H., Gao, Q.: Cryogenic hydrogen uptake of high surface area porous carbon materials activated by potassium hydroxide. Int. J. Hydrogen Energy **35**, 7547–7554 (2010)

Han, S.S., Jung, H., Jung, D.H., Choi, S.-H., Park, N.: Stability of hydrogenation states of graphene and conditions for hydrogen spillover. Phys. Rev. B **85**(155408), 1–5 (2012)

Hirscher, M.: Remarks about spillover and hydrogen adsorption—comments on the contributions of A.V. Talyzin and R.T. Yang. Microporous Mesoporous Mater. **135**, 209–210 (2010)

Ioannatos, G.E., Verykios, X.E.: H_2 storage on single- and multi-walled carbon nanotubes. Int. J. Hydrogen Energy **35**, 622–628 (2010)

Jaramillo, J., Álvarez, P.M., Gómez-Serrano, V.: Oxidation of activated carbon by dry and wet methods. Surface chemistry and textural modification. Fuel Process. Technol. **91**, 1768–1775 (2010)

Jiang, J., Gao, Q., Zheng, Z., Xia, K., Hu, J.: Enhanced room temperature hydrogen storage capacity of hollow nitrogen-containing carbon spheres. Int. J. Hydrogen Energy **35**, 210–216 (2010)

Jiménez, V., Ramírez-Lucas, A., Sánchez, P., Valverde, J.L., Romero, A.: Improving hydrogen storage in modified carbon materials. Int. J. Hydrogen Energy **37**, 4144–4160 (2012)

Jun, S., Joo, S.H., Ryoo, R., Kruk, M., Jaroniec, M., Liu, Z., Ohsuna, T., Terasaki, O.: Synthesis of new, nanoporous carbon with hexagonally ordered mesostructure. J. Am. Chem. Soc. **122**, 10712–10713 (2000)

Kockrick, E., Schrage, C., Borchardt, L., Klein, N., Rose, M., Senkovska, I., Kaskel, S.: Ordered mesoporous carbide derived carbons for high pressure gas storage. Carbon **48**, 1707–1717 (2010)

Kowalczyk, P., Tanaka, H., Hołyst, R., Kaneko, K., Ohmori, T., Miyamoto, J.: Storage of hydrogen at 303 K in graphite slitlike pores from grand canonical Monte Carlo simulation. J. Phys. Chem. B **109**, 17174–17183 (2005)

Kubas, G.J.: Molecular hydrogen complexes: coordination of a σ bond to transition metals. Acc. Chem. Res. **21**, 120–128 (1988)

Lachawiec, A.J., Yang, R.T.: Isotope tracer study of hydrogen spillover on carbon-based adsorbents for hydrogen storage. Langmuir **24**, 6159–6165 (2008)

Lachawiec, A.J., Yang, R.T.: Reverse spillover of hydrogen on carbon-based nanomaterials: evidence of recombination using isotopic exchange. J. Phys. Chem. C **113**, 13933–13939 (2009)

Lee, S.-Y., Park, S.-J.: Preparation and characterization of ordered porous carbons for increasing hydrogen storage behaviors. J. Solid State Chem. **184**, 2655–2660 (2011)

Lee, S.-Y., Park, S.-J.: Influence of oxygen-functional groups on carbon replicas for hydrogen adsorption. Phys. Status Solidi (a) **209**, 694–697 (2012). doi:10.1002/pssa.201127518

Li, Q., Lueking, A.D.: Effect of surface oxygen groups and water on hydrogen spillover in pt-doped activated carbon. J. Phys. Chem. C **115**, 4273–4282 (2011)

Li, Y., Yang, R.T.: Hydrogen storage on platinum nanoparticles doped on superactivated carbon. J. Phys. Chem. C **111**, 11086–11094 (2007)

Li, Z., Yan, W., Dai, S.: Surface functionalization of ordered mesoporous carbons–a comparative study. Langmuir **21**, 11999–12006 (2005)

Lysenko, N.D., Yaremov, P.S., Shvets, A.V., Il'in, V.G.: Effect of the chemical and structural modification of CMK-3 mesoporous carbon molecular sieve on hydrogen adsorption. Theor. Exp. Chem. **45**, 380–385 (2009)

Lu, A.-H., Li, W.-C., Schmidt, W., Schüth, F.: Template synthesis of large pore ordered mesoporous carbon. Microporous Mesoporous Mater. **80**, 117–128 (2005)

Mitchell, P.C.H., Ramirez-Cuesta, A.J., Parker, S.F., Tomkinson, J., Thompsett, D.: Hydrogen spillover on carbon-supported metal catalysts studied by inelastic neutron scattering. surface vibrational states and hydrogen riding modes. J. Phys. Chem. B **107**, 6838–6845 (2003)

Nishihara, H., Hou, P.-X., Li, L.-X., Ito, M., Uchiyama, M., Kaburagi, T., Ikura, A., Katamura, J., Kawarada, T., Mizuuchi, K., Kyotani, T.: High-pressure hydrogen storage in zeolite-templated carbon. J. Phys. Chem. C **113**, 3189–3196 (2009)

Niu, J., Rao, B.K., Jena, P.: Binding of hydrogen molecules by a transition-metal ion. Phys. Rev. Lett. **68**, 2277–2280 (1992)

Panella, B., Hirscher, M., Roth, S.: Hydrogen adsorption in different carbon nanostructures. Carbon **43**, 2209–2214 (2005)

Prins, R.: Hydrogen spillover Facts and fiction. Chem. Rev. **112**, 2714–2738 (2012)

Psofogiannakis, G.M., Froudakis, G.E.: DFT study of hydrogen storage by spillover on graphite with oxygen surface groups. J. Am. Chem. Soc. **131**, 15133–15135 (2009)

Psofogiannakis, G.M., Steriotis, T.A., Bourlinos, A.B., Kouvelos, E.P., Charalambopoulou, G.C., Stubos, A.K., Froudakis, G.E.: Enhanced hydrogen storage by spillover on metal-doped carbon foam: an experimental and computational study. Nanoscale **3**, 933–936 (2011)

Ryoo, R., Joo, S.H., Kruk, M., Jaroniec, M.: Ordered Mesoporous Carbons. Adv. Mater. **13**, 677–681 (2001)

Ryoo, R., Joo, S.H., Jun, S.: Synthesis of highly ordered carbon molecular sieves via template-mediated structural transformation. J. Phys. Chem. B **103**, 7743–7746 (1999)

Salvador, F., Montero, J., Sánchez-Montero, M.J., Izquierdo, C.: Mechanism of heterogeneous adsorption in the storage of hydrogen in carbon fibers activated with supercritical water and steam. Int. J. Hydrogen Energy **36**, 7567–7579 (2011)

Shin, H.J., Ryoo, R., Kruk, M., Jaroniec, M.: Modification of SBA-15 pore connectivity by high-temperature calcination investigated by carbon inverse replication. Chem. Commun. **1**, 349–350 (2001)

Stein, B.A., Wang, Z., Fierke, M.A.: Functionalization of porous carbon materials with designed pore architecture. Adv. Mater. **21**, 265–293 (2009)

Stetson, N. T.: Hydrogen storage overview. DoE Annual Merit Review and Peer Evaluation Meeting (2012)

Takagi, H., Hatori, H., Yamada, Y.: Reversible adsorption/desorption property of hydrogen on carbon surface. Carbon **43**, 3037–3039 (2005)

Texier-Mandoki, N., Dentzer, J., Piquero, T., Saadallah, S., David, P., Vix-Guterl, C.: Hydrogen storage in activated carbon materials: role of the nanoporous texture. Carbon **42**, 2744–2747 (2004)

Toebes, M.L., Van Dillen, J.A., De Jong, K.P.: Synthesis of supported palladium catalysts. J. Mol. Catal. A: Chem. **173**, 75–98 (2001)

Tsao, C.-S., Liu, Y., Li, M., Zhang, Y., Leao, J.B., Chang, H.-W., Yu, M.-S., Chen, S.-H.: Neutron scattering methodology for absolute measurement of room-temperature hydrogen storage capacity and evidence for spillover effect in a pt-doped activated carbon. J. Phys. Chem. Lett. **1**, 1569–1573 (2010)

Wang, L., Yang, F.H., Yang, R.T.: Hydrogen storage properties of b- and n-doped microporous carbon. Am. Inst. Chem. Eng. **55**, 1823–1833 (2009)

Wang, L., Yang, R.T.: Hydrogen storage on carbon-based adsorbents and storage at ambient temperature by hydrogen spillover. Catal. Rev. **52**, 411–461 (2010)

Wang, L., Yang, R.T.: Molecular hydrogen and spiltover hydrogen storage on high surface area carbon sorbents. Carbon **50**, 3134–3140 (2012)

Wang, Z., Yang, F.H., Yang, R.T.: Enhanced hydrogen spillover on carbon surfaces modified by oxygen plasma. J. Phys. Chem. C **114**, 1601–1609 (2010)

Xia, K., Gao, Q., Song, S., Wu, C., Jiang, J., Hu, J., Gao, L.: CO_2 activation of ordered porous carbon CMK-1 for hydrogen storage. Int. J. Hydrogen Energy **33**, 116–123 (2008)

Xia, K., Gao, Q., Wu, C., Song, S., Ruan, M.: Activation, characterization and hydrogen storage properties of the mesoporous carbon CMK-3. Carbon **45**, 1989–1996 (2007)

Yang, F.H., Lachawiec, A.J., Yang, R.T.: Adsorption of spillover hydrogen atoms on single-wall carbon nanotubes. J. Phys. Chem. B **110**, 6236–6244 (2006)

Yang, R.T., Chen, H., Diraimondo, T.R., Lachawiec, A.J., Stuckert, N., Wang, L., Wang, Y., et al.: Hydrogen Storage at Ambient Temperature by the Spillover Mechanism. DoE Sci. Tech. Inf. (2011a). doi:10.2172/1004576

Yang, S.J., Im, J.H., Nishihara, H., Jung, H., Lee, K., Kyotani, T., Park, C.R.: General relationship between hydrogen adsorption capacities at 77 and 298 k and pore characteristics of the porous adsorbents. J. Phys. Chem. C **116**, 10529–10540 (2012)

Yang, Y., Brown, C.M., Zhao, C., Chaffee, A.L., Nick, B., Zhao, D., Webley, P.A., Schalch, J., Simmons, J.M., Liu, Y., Her, J.-H., Buckley, C.E., Sheppard, D.A.: Micro-channel development and hydrogen adsorption properties in templated microporous carbons containing platinum nanoparticles. Carbon **49**, 1305–1317 (2011b)

Zhao, D., Feng, J., Huo, Q., Melosh, N., Fredrickson, G.H., Chmelka, B.F., Stucky, G.: Triblock copolymer syntheses of mesoporous silica with periodic 50–300 angstrom pores. Science **279**, 548–552 (1998a)

Zhao, D., Huo, Q., Feng, J., Chmelka, B.F., Stucky, G.D.: Nonionic triblock and star diblock copolymer and oligomeric surfactant syntheses of highly ordered, hydrothermally stable, mesoporous silica structures. J. Am. Chem. Soc. **120**, 6024–6036 (1998b)

Zhao, W., Fierro, V., Zlotea, C., Izquierdo, M.T., Chevalier-César, C., Latroche, M., Celzard, A.: Activated carbons doped with Pd nanoparticles for hydrogen storage. Int. J. Hydrogen Energy **37**, 5072–5080 (2012)

Zheng, Z., Gao, Q., Jiang, J.: High hydrogen uptake capacity of mesoporous nitrogen-doped carbons activated using potassium hydroxide. Carbon **48**, 2968–2973 (2010)